## Supplementary S1. Procedures

*Supplementary S1.1. Calibration Procedure for thermal conductivity detector (TCD)*

For calibrating the TCD hydrogen sensitivity, 13.00 mg of CuO (99.9995 %, Alfa Aesar) was filled into the reactor and flushed with helium flow (30 ml/min) at room temperature until the signal stabilized. Then, it was heated with hydrogen in argon (1.99 %, $c_{H_2}$ =2 %) at a heating rate of $\beta$ =10 K/min and flow rate of $F$ =30 ml/min from 35 °C to 800 °C. The hydrogen consumption was measured using the TCD and mass spectrometer, correlating the area of signal change with the stoichiometrically required amount of hydrogen from equation (S1).

$$Cu^{II}O + H_2 \longrightarrow Cu^0 + H_2O \tag{S1}$$

The calibration factor was calculated using three independent experiments as in section Supplementary S2.1.

## Supplementary S2. Calculations

*Supplementary S2.1. Calculation of $C_f$ for the TPDRO Measurements*

The calibration factor $C_f$ of the TPDRO was determined based on three independent calibration measurements using CuO.

$$\bar{C_f} = \frac{C_{f1} + C_{f2} + C_{f3}}{3} \tag{S2}$$

$$C_{fn} = \frac{m(\mathrm{CuO})}{M(\mathrm{CuO}) \cdot A_{\mathrm{TCD}}} \tag{S3}$$

Here, $\Delta m(\mathrm{CuO}) = \pm\, 0.0001$ g, and M(CuO) and $A_{\mathrm{TCD}}$ are considered error-free:

$$\Delta\bar{C_f} = \sqrt{\left(\frac{1}{3}\right)^2 (\Delta C_{f1})^2 + \left(\frac{1}{3}\right)^2 (\Delta C_{f2})^2 + \left(\frac{1}{3}\right)^2 (\Delta C_{f3})^2} \tag{S4}$$

$$\Delta\bar{C_f} = \frac{1}{3}\sqrt{(\Delta C_{f1})^2 + (\Delta C_{f2})^2 + (\Delta C_{f3})^2} \tag{S5}$$

$$\Delta C_{fn} = \sqrt{\left(\frac{\delta C_{fn}}{\delta m(\mathrm{CuO})}\right)^2 \Delta m_n(\mathrm{CuO})^2} \tag{S6}$$

$$\Delta C_{fn} = \sqrt{\left(\frac{1}{M(\mathrm{CuO}) \cdot A_{\mathrm{TCD}}}\right)^2 \Delta m_n(\mathrm{CuO})^2} \tag{S7}$$

$$\begin{aligned}\Delta\bar{C_f} = \frac{1}{3}\Bigg\{ &\left(\frac{1}{M(\mathrm{CuO}) \cdot A_{\mathrm{TCD}-1}}\right)^2 \Delta m_1(\mathrm{CuO})^2 \\ &+ \left(\frac{1}{M(\mathrm{CuO}) \cdot A_{\mathrm{TCD}-2}}\right)^2 \Delta m_2(\mathrm{CuO})^2 \\ &+ \left(\frac{1}{M(\mathrm{CuO}) \cdot A_{\mathrm{TCD}-3}}\right)^2 \Delta m_3(\mathrm{CuO})^2 \Bigg\}^{\frac{1}{2}}\end{aligned} \tag{S8}$$

Table S1 presents the experimentally determined values.

**Table S1.** Experimental data for determining the calibration factor $C_f$. Experimental conditions $\dot{V}_{Setpoint} = 25$ mL/min, $\beta = 10$ K/min with 1.99 Vol % $H_2$/Ar.

| Experiment | $m$(CuO) g | $n$(CuO) mmol | $A$(TCD) mVs | $C_f$ mmol/mVs |
|---|---|---|---|---|
| JH-272 | $0.0100 \pm 0.0002$ | 0.1257 | 6 883 481.66 | $(1.83 \pm 0.37) \times 10^{-8}$ |
| JH-289-2 | $0.0105 \pm 0.0002$ | 0.1320 | 9 337 870.52 | $(1.41 \pm 0.27) \times 10^{-8}$ |
| JH-289-1 | $0.009\,970 \pm 0.000\,002$ | 0.1253 | 7 125 709.78 | $(1.76 \pm 0.35) \times 10^{-8}$ |

This resulted in a calibration factor $C_f$ of $(1.66 \pm 0.02) \times 10^{-8}$ mmol/(mV s).

*Supplementary S2.2. Calculation of surface atoms in bimetallic metal particles*

As the chemisorption properties of bimetallic materials are unpredictable, the number of surface atoms ($N_{\text{Surface Atoms}}$) was calculated based on the median ($d_{\text{Particle}}$) of the particle size distributions from the TEM measurements or crystallite size from the XRD measurements.

As the turnover frequency (TOF) refers to the number of surface atoms in the reaction, various assumptions can be made regarding their calculation. In the case of maximal dispersion ($D = 1$), all metal atoms in the catalyst are available for the reaction. In this case, all atoms are located directly at the interface of the heterogeneous catalyst with the liquid phase in the reaction. This case is described hereinafter as $TOF_{\text{th}}$. The number of surface atoms was identical to the metal loadings of the catalyst found in the inductive coupled plasma (ICP) measurements, denoted as $w_{\text{ICP}}$. Hence, this case was calculated using equation (S10).

$$N_{\text{Surface Atoms}} = m_{\text{Cat}} \cdot \left( \frac{w_{\text{ICP}_i}}{M_{\text{Metal}_i}} + \frac{w_{\text{ICP}_j}}{M_{\text{Metal}_j}} \right) \cdot N_{\text{A}} \tag{S9}$$

Consequently, equations (1), (2) and (S9) leads to equation (S10), which serves as the basis for the calculation of $TOF_{th}$ in Table 6.

$$TOF_{\text{th}} = \frac{c_{i_{\text{R}}}^{i-\text{ButOH}} \cdot V_{\text{R}}}{m_{\text{Cat}} \cdot \left( \frac{w_{\text{ICP}_i}}{M_{\text{Metal}_i}} + \frac{w_{\text{ICP}_j}}{M_{\text{Metal}_j}} \right) \cdot t_{\text{Reaction}}} \tag{S10}$$

As the XRD and STEM measurements indicate that the dispersion is not $D = 1$, the number of actual surface atoms must be estimated. For this purpose, the particle is divided into two components: the core and the surface. The surface atoms constitute the outermost atomic layer of the particle, whereas the atoms underneath form the particle core.

The metal particles are treated approximately as spheres. The cross-sectional area of the atom for substance $i$ or $j$ is defined by its covalent radius $r_{i(j)} = \frac{d_{i(j)}}{2}$. The substance composition determined by ICP–OES $x_i(j)$ for substance $i$ or $j$ is given as a percentage.

$$N_{\text{Surface Atoms}} = (N_{\text{Atoms/Particle}} - N_{\text{Core Atoms/Particle}}) \cdot N_{\text{Particle}} \tag{S11}$$

The number of metal particles ($N_{\text{Particle}}$) is determined from the loading ($w_{\text{Metal}}$) obtained by ICP–OES and the calculated particle mass ($m_{\text{Particle}}$).

$$N_{\text{Particle}} = \frac{m_{\text{Catalyst}} \cdot w_{\text{Metal}}}{m_{\text{Particle}}} \tag{S12}$$

The particle mass was derived from the particle density ($\rho_{\text{Particle}}$) and particle volume ($V_{\text{Particle}}$), which is calculated using the median particle diameter.

$$m_{\text{Particle}} = \rho_{\text{Particle}} \cdot V_{\text{Particle}} \tag{S13}$$

$$V_{\text{Particle}} = \frac{4}{3}\pi \left( \frac{d_{\text{Particle}}}{2} \right)^3 \tag{S14}$$

For bimetallic materials, the expansion of the lattice constants $a_{ij}$ must be considered according to Vegard's rule. $a_{i(j)}$ represents the lattice constant for substances $i$ or $j$. This was divided by the mass of the elementary cell $m_{\text{EC}}$. The mass of the elementary cell was calculated for the cubic face-centered arrangement for four atoms ($N_{\text{Atoms}}^{\text{fcc}} = 4$), which were weighted according to the substance compositions $x_{i(j)}$ found by ICP–OES for substances $i$ and $j$.

$$\rho_{\text{Particle}} = \frac{m_{\text{EC}}}{V_{\text{EC}}} \tag{S15}$$

$$m_{\text{EC}} = (m_i \cdot x_i + m_j \cdot x_j) \cdot N_{\text{Atoms}}^{\text{fcc}} \tag{S16}$$

$$V_{\text{EC}} = (x_i \cdot a_i + (1 - x_i) \cdot a_j)^3 \tag{S17}$$

For the cubic body-centered crystal structure, $N_{\text{Atoms}}^{\text{bcc}} = 2$ was used. The number of atoms in a particle $N_{\text{Atoms/Particle}}$ was calculated by the ratio determined by the particle volume.

$$N_{\text{Atoms/Particle}} = \frac{\frac{4}{3}\pi\left(\frac{d_{\text{Particle}}}{2}\right)^3 \cdot \rho_{\text{Particle}}}{M_{\text{Particle}}} \cdot N_{\text{A}} \tag{S18}$$

The number of core atoms $N_{CoreAtoms}$ were calculated by subtracting the outer atomic layer ($4r_{Atom}$) from the particle diameter.

$$N_{\text{Core Atoms/Particle}} = \frac{\frac{4}{3}\pi\left(\frac{d_{\text{Particle}} - 4r_{\text{Atom}}}{2}\right)^3 \cdot \rho_{\text{Particle}}}{M_{\text{Particle}}} \cdot N_{\text{A}} \tag{S19}$$

Thus, equation (S11) is transformed into equation (S20).

$$N_{\text{Surface Atoms}} = \frac{4}{3}\pi\frac{\rho_{\text{Particle}}}{M_{\text{Particle}}} \cdot N_{\text{A}} \cdot N_{\text{Particle}}\left(\left(\frac{d_{\text{Particle}}}{2}\right)^3 - \left(\frac{d_{\text{Particle}} - 4r_{\text{Atom}}}{2}\right)^3\right) \tag{S20}$$

$$= \frac{1}{6}\frac{\pi\rho_{\text{Particle}}}{M_{\text{Particle}}} \cdot N_{\text{A}} \cdot N_{\text{Particle}} \cdot \left(d_{\text{Particle}}^3 - (d_{\text{Particle}} - 4r_{\text{Atom}})^3\right) \tag{S21}$$

Using equations (S12) to (S14) yields:

$$N_{\text{Surface Atoms}} = \frac{N_{\text{A}} \cdot m_{\text{Cat}} \cdot w_{\text{ICP}}}{M_{\text{Particle}}} \cdot \left(1 - \frac{(d_{\text{Particle}} - 4r_{\text{Atom}})^3}{d_{\text{Particle}}^3}\right) \tag{S22}$$

The term $\frac{N_{\text{A}} \cdot m_{\text{Cat}} \cdot w_{\text{ICP}}}{M_{\text{Particle}}}$ describes the total number of metal atoms on the catalyst used in the experiment. The term $\frac{(d_{\text{Particle}} - 4r_{\text{Atom}})^3}{d_{\text{Particle}}^3}$ describes the ratio of the particle diameters of the core atoms to the complete particle diameter. Thus, the difference calculates the sum of surface atoms on the catalyst material used in the experiment. The covalent atomic radii of the metals used are listed in Table S2.

**Table S2.** Tabulated values for the crystallographic lattice parameters.

| Metal | $a$<br>pm | $r_{\text{Atom}}$<br>pm | M<br>u | Structure type |
|---|---|---|---|---|
| α-Fe | 286.645 [63] | 126 [64, S. 2146] | 55.845 [63] | bcc [63] |
| Ni | 351.68 [65] | 124.6 [64, S. 2148] | 58.693 [63] | fcc [65] |
| Pd | 393.2 [66] | 137.6 [64, S. 2148] | 106.400 [66] | fcc [66] |
| Pt | 392.32 [67] | 137.3 [64, S. 2148] | 195.090 [67] | fcc [67] |
| Cu | 359.42 [37] | 127.8 [64, S. 2148] | 63.5500 [37] | fcc [68] |

## Supplementary S3. Tables

**Table S3.** Tabular listing of the feed for bimetallic catalysts prepared by impregnation. All values are given in g.

| | $Cu(NO_3)_2 \cdot 2.5\,H_2O$ | $Ni(NO_3)_2 \cdot 6\,H_2O$ | $Fe(NO_3)_3 \cdot 9\,H_2O$ | $[Pt(NH_3)_4](NO_3)_2$ | $[PdCl_4](NH_4)_2$ | $H_2O$ | Activated Carbon |
|---|---|---|---|---|---|---|---|
| Cu/C | 0.9160 | – | – | – | – | 2.5000 | 4.8700 |
| Fe/C | – | – | 1.8100 | – | – | 1.7500 | 4.9580 |
| Ni/C | – | 1.2380 | – | – | – | 2.1000 | 4.8800 |
| $Cu_{99}Fe_1/C$ | 0.9045 | – | 0.0179 | – | – | 2.9000 | 5.6800 |
| $Cu_{99}Ni_1/C$ | 0.9040 | 0.0121 | – | – | – | 2.7500 | 5.2401 |
| $Fe_{99}Pd_1/C$ | – | – | 1.7920 | – | 0.0071 | 2.1500 | 4.8840 |
| $Fe_{99}Pt_1/C$ | – | – | 1.7910 | 0.0048 | – | 2.2500 | 4.9500 |
| $Ni_{99}Pt_1/C$ | – | 1.2251 | – | 0.0051 | – | 2.3500 | 4.8780 |

**Table S4.** ICP–OES determined stoichiometric ratios of the impregnation catalysts.

| No. | Composition | $w_{Metal}$ | $x$ in % | | | | |
|---|---|---|---|---|---|---|---|
| | EXPECTED | % | Ni | Cu | Fe | Pt | Pd |
| 1 | 5% $Ni_{99}Pt_1/C$ | $3.61 \pm 0.03$ | 99.77 | – | – | 0.23 | – |
| 2 | 5% $Cu_{99}Ni_1/C$ | $3.86 \pm 0.05$ | 0.03 | 99.97 | – | – | – |
| 3 | 5% $Cu_{99}Fe_1/C$ | $4.51 \pm 0.27$ | – | 99.94 | 0.06 | – | – |
| 4 | 5% $Fe_{99}Pd_1/C$ | $4.06 \pm 0.37$ | – | – | 99.62 | – | 0.38 |
| 5 | 5% $Fe_{99}Pt_1/C$ | $3.48 \pm 0.15$ | – | – | 99.59 | 0.41 | – |

## Supplementary S4. Graphs

*Supplementary S4.1. Particle size distribution*

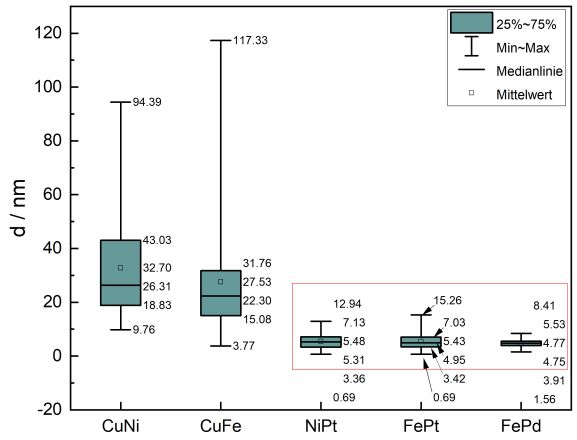


**Figure S1.** Box plot of the particle distribution from the STEM images for the catalysts $Ni_{99}Pt_1/C$, $Cu_{99}Ni_1/C$, $Cu_{99}Fe_1/C$, $Fe_{99}Pt_1/C$, and $Fe_{99}Pd_1/C$. The box represents the second and third quartiles and the median. The average is represented by a small square. The whiskers represent the minima and maxima of the particle sizes. The red box is shown in detail in figure S2.

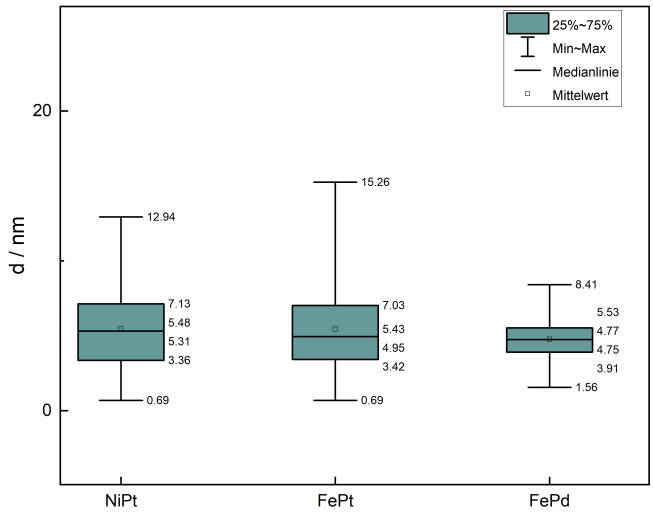


**Figure S2.** Box plot of the particle distribution from the STEM images for the catalysts $Ni_{99}Pt_1/C$, $Fe_{99}Pt_1/C$, and $Fe_{99}Pd_1/C$. The box represents the second and third quartiles and the median. The average is represented by a small square. The whiskers represent the minima and maxima of the particle sizes.

*Supplementary S4.2. Deconvoluted TPR measurements*

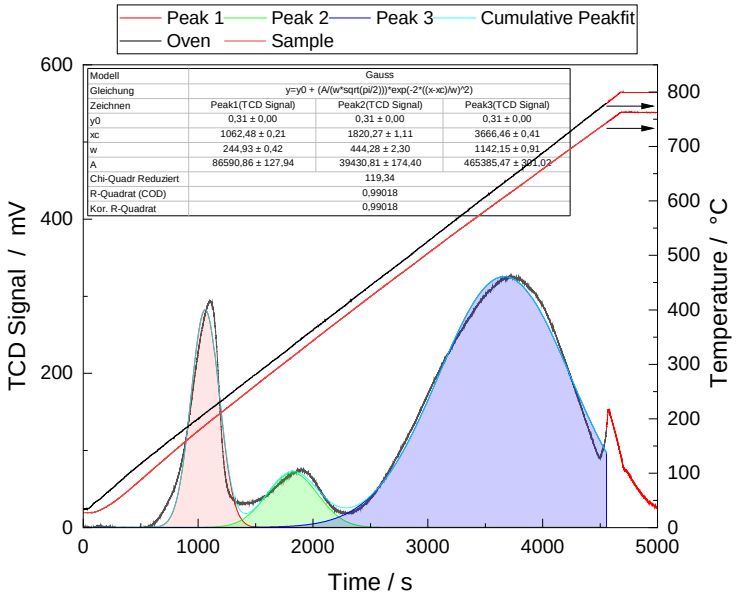


**Figure S3.** TPR Profile of the Cu/C catalyst with peak decomposition using *Gaussian* functions. Measurement conditions: $m_{\mathrm{Cat}}$=48.9 mg, 2 %$H_2$ in argon, $\dot{V} = 30\,\mathrm{mL/min}$; $\beta = 10\,\mathrm{K/min}$. The calibration factor $f_{\mathrm{WLD}} = 9.192\,09 \times 10^{-8}\,\mathrm{mmol\,s/mV}$ was determined with CuO 99.9995 % purity. Peak decomposition was performed using the Peak Fitting Tool of OriginPro software, Version 2021. OriginLab Corporation, Northampton, MA, USA. The baseline was set to 0.31 mV. Data above temperatures of 779 °C were masked to reduce the influence of the slowed heating rate.

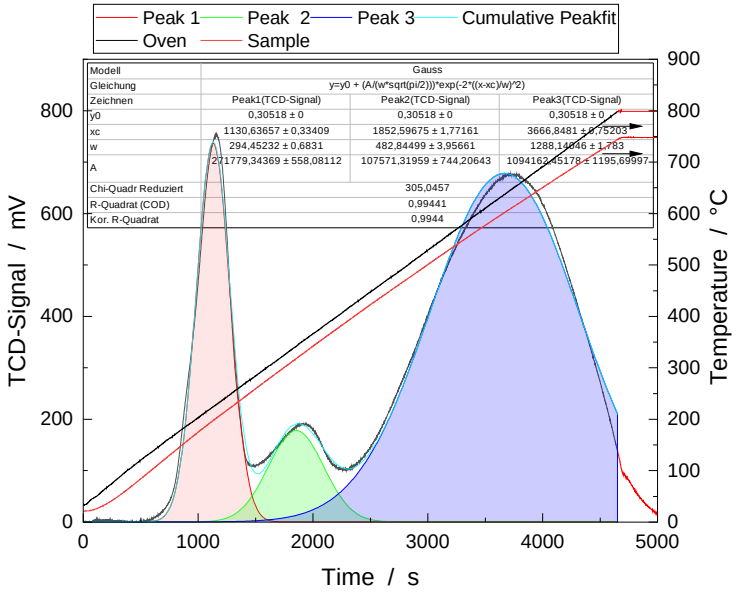


**Figure S4.** TPR profile of the CuNi/C catalyst with peak decomposition using *Gaussian* functions. Measurement conditions: $m_{\mathrm{Cat}}$=88.3 mg, 2 %$H_2$ in argon, $\dot{V} = 30\,\mathrm{mL/min}$; $\beta = 10\,\mathrm{K/min}$. The calibration factor $f_{\mathrm{WLD}} = 9.192\,09 \times 10^{-8}\,\mathrm{mmol\,s/mV}$ was determined with CuO 99.9995 % purity. Peak decomposition was performed using the Peak Fitting Tool of OriginPro software, Version 2021. OriginLab Corporation, Northampton, MA, USA. The baseline was set to 0.31 mV. Data above temperatures of 779 °C were masked to reduce the influence of the slowed heating rate.

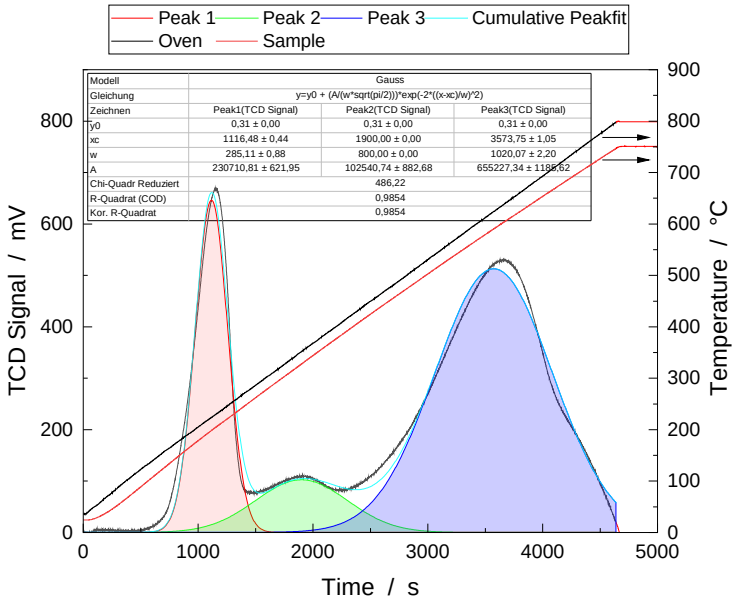


**Figure S5.** TPR profile of the CuFe/C catalyst with peak decomposition using *Gaussian* functions. Measurement conditions: $m_{\mathrm{Cat}}$=80.7 mg, 2 %$H_2$ in argon, $\dot{V} = 30\,\mathrm{mL/min}$; $\beta = 10\,\mathrm{K/min}$. The Calibration factor $f_{\mathrm{WLD}} = 9.192\,09 \times 10^{-8}\,\mathrm{mmol\,s/mV}$ was determined with CuO 99.9995 % purity. Peak decomposition was performed using the Peak Fitting Tool of OriginPro software, Version 2021. OriginLab Corporation, Northampton, MA, USA. The baseline was set to 0.31 mV. Data above temperatures of 779 °C were masked to reduce the influence of the slowed heating rate. To obtain a stable solution, the values $xc$ and $w$ were fixed for for Peak 2.

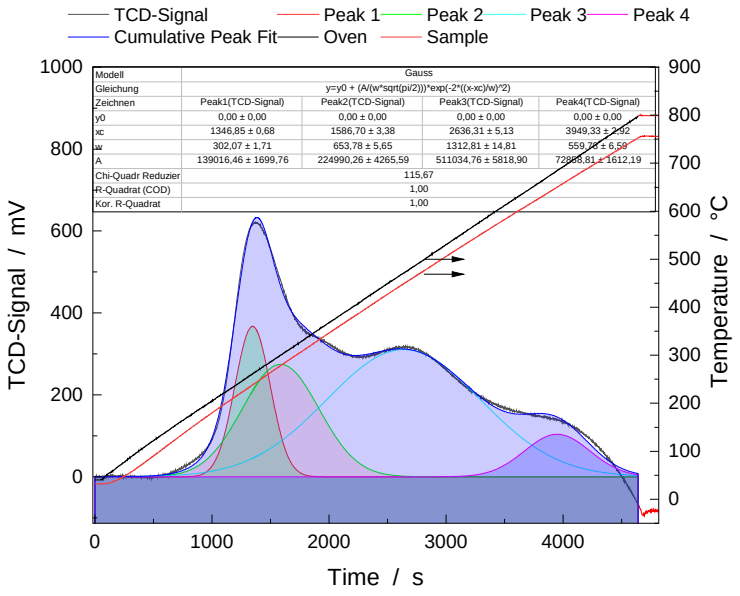


**Figure S6.** TPR profile of the Ni/C catalyst with peak deconvolution using *Gaussian* functions. Measurement conditions: $m_{\mathrm{Cat}}$=80.7 mg, 2 %$H_2$ in argon, $\dot{V} = 30\,\mathrm{mL/min}$; $\beta = 10\,\mathrm{K/min}$. The calibration factor $f_{\mathrm{WLD}}$=$9.192\,09 \times 10^{-8}\,\mathrm{mmol\,s/mV}$ was determined with CuO 99.9995 % purity. Peak decomposition was performed using the Peak Fitting Tool of OriginPro software, Version 2021. OriginLab Corporation, Northampton, MA, USA. The baseline was set to 0.00 mV. Data above temperatures of 798 °C were masked to reduce the influence of the slowed heating rate.

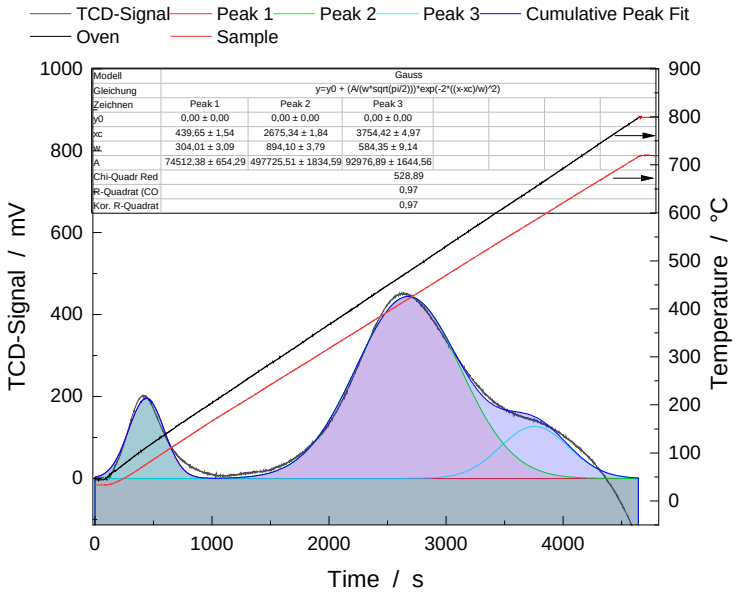


**Figure S7.** TPR profile of the NiPt/C catalyst with peak deconvolution using *Gaussian* functions. Experimental conditions: $m_{\mathrm{Cat}} = 80.7\,\mathrm{mg}$, 2 %$H_2$ in argon, $\dot{V} = 30\,\mathrm{mL/min}$; $\beta = 10\,\mathrm{K/min}$. The calibration factor $f_{\mathrm{WLD}}$=9.192 09 $\times\ 10^{-8}\,\mathrm{mmol\,s/mV}$ was determined with CuO 99.9995 % purity. Peak decomposition was performed using the peak fitting tool of the software *OriginPro*, Version 2021, OriginLab Corporation, Northampton, MA, USA. The baseline was set at 0.00 mV. Data above temperatures of 798 °C were masked to reduce the influence of the slowed heating rate.

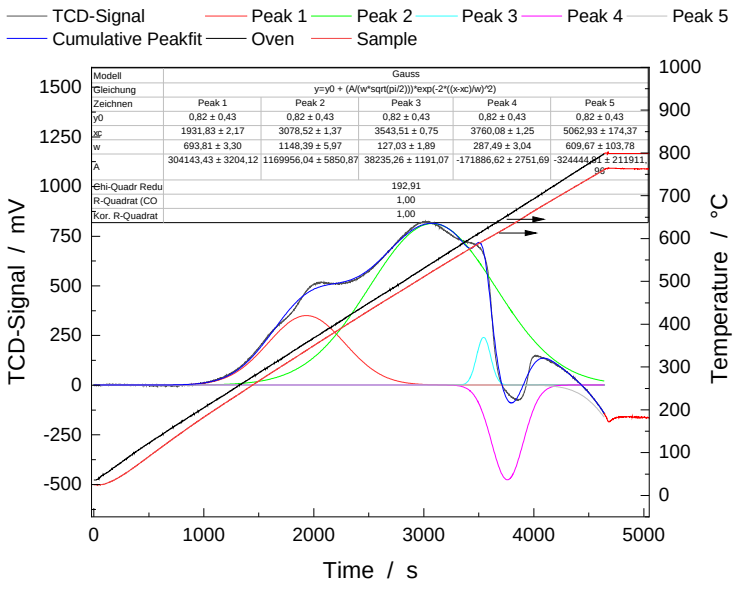


**Figure S8.** TPR profile of the Fe/C catalyst with peak deconvolution using *Gaussian* functions. Experimental conditions: $m_{\mathrm{Cat}} = 89.4\,\mathrm{mg}$, 2 %$H_2$ in argon, $\dot{V} = 30\,\mathrm{mL/min}$; $\beta = 10\,\mathrm{K/min}$. The calibration factor $f_{\mathrm{WLD}} = 9.192\,09 \times 10^{-8}\,\mathrm{mmol\,s/mV}$ was determined with CuO 99.9995 % purity. Peak decomposition was performed using the peak fitting tool of the software *OriginPro*, Version 2021, OriginLab Corporation, Northampton, MA, USA. The baseline was set at 0.00 mV. Data above temperatures of 798 °C were masked to reduce the influence of the slowed heating rate.

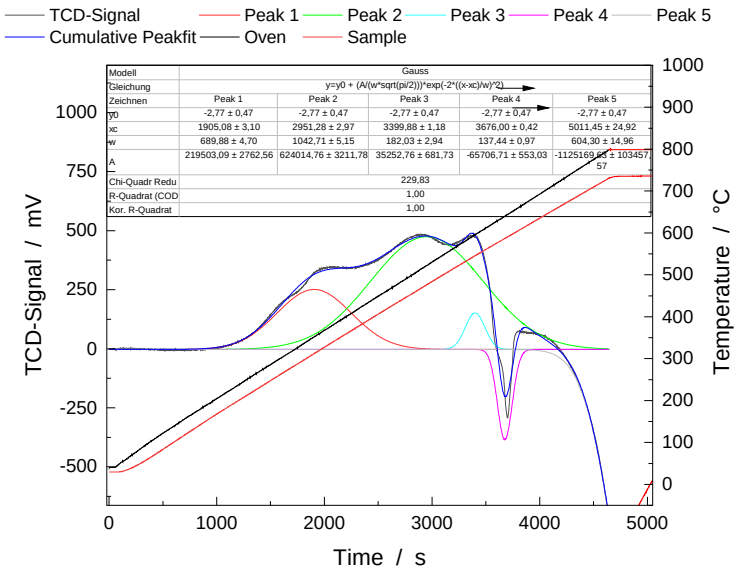


**Figure S9.** TPR profile of the FePd/C catalyst with peak deconvolution using *Gaussian* functions. Experimental conditions: $m_{Cat} = 54.1\,\text{mg}$, 2 %$H_2$ in argon, $\dot{V} = 30\,\text{mL/min}$; $\beta = 10\,\text{K/min}$. The calibration factor $f_{\text{WLD}} = 9.192\,09 \times 10^{-8}\,\text{mmol\,s/mV}$ was determined with CuO 99.9995 % purity. Peak decomposition was performed using the peak fitting tool of the software *OriginPro*, Version 2021, OriginLab Corporation, Northampton, MA, USA. The baseline was set at 0.00 mV. Data above temperatures of 798 °C were masked to reduce the influence of the slowed heating rate.

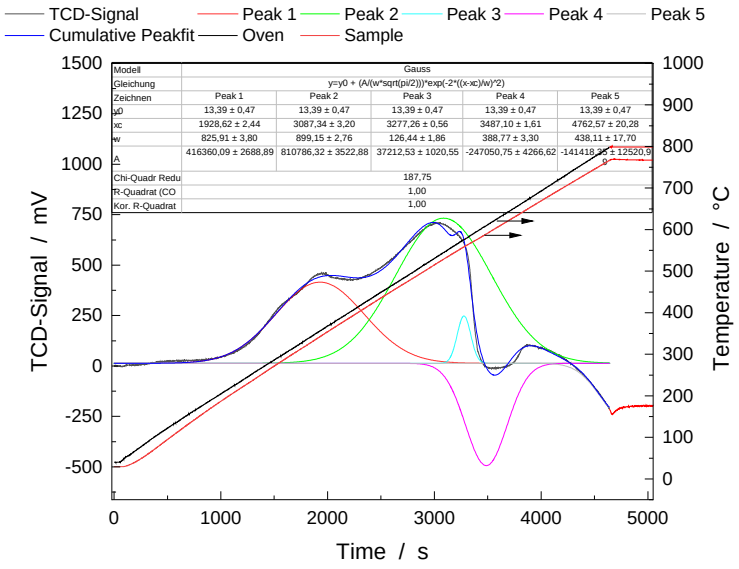


**Figure S10.** TPR profile of the FePt/C catalyst with peak deconvolution using *Gaussian* functions. Experimental conditions: $m_{\text{Cat}} = 81.8\,\text{mg}$, 2 %$H_2$ in argon, $\dot{V} = 30\,\text{mL/min}$; $\beta = 10\,\text{K/min}$. The calibration factor $f_{\text{WLD}} = 9.192\,09 \times 10^{-8}\,\text{mmol\,s/mV}$ was determined with CuO 99.9995 % purity. Peak decomposition was performed using the peak fitting tool of the software *OriginPro*, Version 2021, OriginLab Corporation, Northampton, MA, USA. The baseline was set at 0.00 mV. Data above temperatures of 798 °C were masked to reduce the influence of the slowed heating rate.